Influence of Initial and Boundary Conditions on Vortex Ring Development

J. Z. Irdmusa* and C. A. Garris†
George Washington University, Washington, D.C.

Abstract

THIS paper presents the results of an experimental investigation comparing the mass and energy content of fully formed laminar vortex rings in air with that of the original pulse that generated them for a variety of initial and boundary conditions. In particular, the fractional entrainment of mass and the partition of initial energy between kinetic energy of translation and kinetic energy of rotation are studied. It is found that these characteristics depend strongly on the boundary conditions. A technique is presented which enables calculation of kinetic energy of rotation from motion picture sequences. The ratio of characteristic translational speed to characteristic rotational speed is shown to be a useful parameter for correlation of data. Data on vortex size and speed are presented using this correlation, and it is seen that all data, regardless of initial and boundary conditions, fall on a single curve. A theoretical curve is derived, and it is seen that the data compare well with it.

Contents

In many applications utilizing nonsteady flow, it is of importance to understand the mechanisms of mass, momentum, and energy exchange between a primary flow and a secondary flow. The present work attempts to shed light on such mechanisms by ultilizing a simple example: the formation of vortex rings.

A sketch of the system under study is shown in Fig. 1. We consider that, at time $t=0$, a uniform pulse is initiated with velocity $u_j(t)$ for a duration T_p through a chimney of height H and diameter D_0. Note that, when $H=0$, we have a simple orifice. After a certain period of time, the pulse becomes a fully formed vortex ring of diameter D which propagates at a speed U. The nature of the vortex ring will depend on the boundary conditions (H, D_0) and on the initial conditions $[u_j(t), T_p]$.

Since all of the vorticity essential to the existence of a vortex is generated in boundary layers prior to formation, different geometries will produce different amounts of vorticity. Furthermore, in the case of the simple orifice, vorticity of opposite sense is generated on the outside of the orifice by the boundary layer formed from the entrained flow, passing over the solid surface, thereby impeding the influx of entrained flow and diminishing the net available vorticity. These effects will result in the generation of vortices with different sizes and different propagation speeds, as well as differences in internal flowfields.

In the experimental investigation, vortex rings were generated in still air for various sizes of simple orifices and chimneys by means of a large loudspeaker energized by a step in voltage, producing a controllable jet-pulse intensity. The pulse intensity and duration were monitored by means of a hot-film anemometer. Oscillographic records of the anemometer trace enable calculation of pulse mass, momentum, and energy by integration. A detailed photographic study comparing each instant of the oscilloscope record with the developing vortex ring at the same instant revealed that the vortex formation entirely occurs during a primary pulse of duration T_p. The anemometer probe was traversed laterally across the orifice, and it was observed that the principal waveform changed little from section to section. Thus, it was indicative that the flow at the exit of the orifice or chimney is reasonably uniform, and a "top-hat" profile can be assumed.

Flow visualization was achieved by introducing cigarette smoke in the primary jet through the loudspeaker enclosure, or by introducing paraffin smoke in the secondary fluid just outside the jet exit. Both methods of flow visualization in conjunction with hot-film anemometer traces were utilized to ensure that the visual boundaries of the vortex corresponded to the actual boundaries. Our results indicated that they did. Furthermore, the smoke was not observed to experience appreciable diffusion within the time scale of the motion. Hence, the mass, momentum, and energy of the fully formed vortex can be determined by photographic analysis.

The motion and development of the vortex ring was established by means of both multiple-flash open-shutter photography and high-speed motion pictures. A motion-picture sequence of vortex formation is shown in Fig. 2 whereby an emerging slug of primary fluid flattens out, as a rivot, when it impinges upon the initially stagnant ambient fluid. It then captures ambient fluid in a core, separates from the source, and propagates downstream as a vortex ring, with a relatively constant velocity U and diameter D for a distance exceeding 10 diam before dissipating. Data showed that chimney-generated vortices tended to be slower and larger than orifice-generated vortices for a given source intensity and source diameter.

In order to correlate the data and gain physical insight into the processes involved, universal dimensionless scaling parameters were sought by means of simplified theoretical reasoning. The phenomenon of vortex formation shown in Fig. 2 is suggestive of the process of inelastic particle collisions common in elementary physics. In such processes, mo-

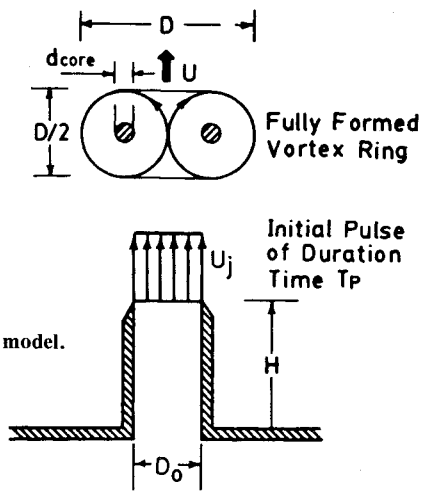

Fig. 1 Mathematical model.

Received Oct. 30, 1984; synoptic received June 20, 1986. Full paper available from National Technical Information Service, Springfield, VA 22151, at the standard price (available upon request).

*Research Assistant.
†Professor of Engineering.

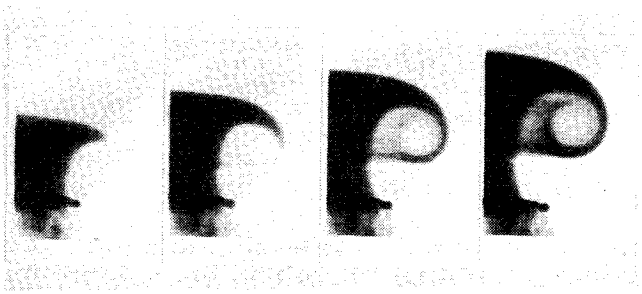

Fig. 2 Motion-picture sequence of smoke filament in the process of surrounding the vortex core.

mentum is conserved. In the present problem, if it is assumed that viscous effects are negligible and one disregards the wake behind the vortex, momentum would likewise be conserved. The momentum carried by the initial pulse of fluid is easily calculated from anemometer traces, and the momentum of the fully formed vortex may be estimated from photographic records. Assuming that the geometry of the vortex is approximated by that shown in Fig. 1, conservation of linear momentum yields

$$DU/\overline{u_j^2}T_p = 2.47(D/D_0)^{-2} \tag{1}$$

or

$$U^* = 2.47D^{*-2} \tag{2}$$

A very useful physical interpretation of the parameter U^* may be obtained from approximation that the initial pulse is a square wave of amplitude u_j (rms). In such case, the circulation Γ is given by

$$\Gamma = \tfrac{1}{2}\overline{u_j^2}T_p \tag{3}$$

Hence

$$U^* = \frac{U}{2\Gamma/D} = \frac{\text{translational speed}}{\text{rotational speed}} \tag{4}$$

The results of this correlation are shown plotted with the theoretical prediction, Eq. (2), in Fig. 3. It is seen that the results indeed approximate the ideal curve. The fact that the data do agree with the theoretical curve suggests that the assumption that the flow surrounding the vortex is approximately irrotational, with D'Alembert's paradox applying, is a reasonable simplification.

An attempt was made to include data from the literature in the correlation. However, the only reference containing all of the information needed was Sallet.[1] These data were consistent with those of the present work and the theoretical prediction; they are shown by circles in Fig. 3.

Figure 3, in conjunction with Eq. (1), does show that for a given diameter ratio D^* the vortex speed will vary as the mean-square pulse intensity, and that for a given pulse intensity the vortex speed varies inversely as the cube of the vortex diameter. The graph also shows the previously discussed result that the chimney vortices are larger and slower than the orifice vortices.

The total kinetic energy of a system of particles is the sum of the kinetic energy of the mass center (as if the total mass of the system were concentrated there) and the total kinetic energy of the particles caused by the relative motion with respect to the mass center, viz., translational plus rotational kinetic energies. The translational kinetic energy of vortices can easily be estimated from photographic records, and the initial kinetic energy from anemometer records.

Figure 4 shows the ratio of translational kinetic energy of the vortex to the initial kinetic energy of the jet vs U^*. Although there is substantial scatter, all data appear to lie on a single curve. The chimney vortices show a much lower fraction of translational kinetic energy than the orifice vortices. This suggests that the chimney vortices have proportionately more kinetic energy of rotation, neglecting losses. Note that this observation is consistent with the physical interpretation of U^* as being the ratio of translational to rotational characteristic velocities, since low U^* should imply high rotation, and vice versa.

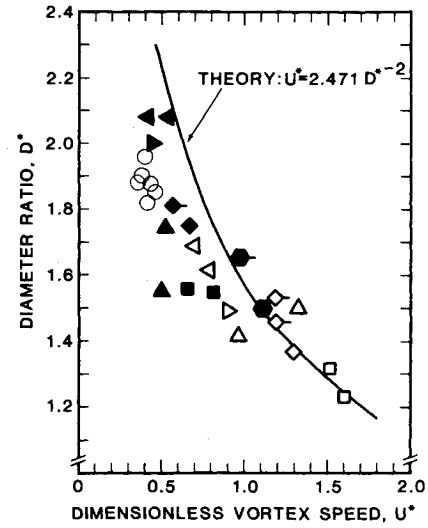

Fig. 3 Ratio of vortex diameter to exit diameter vs dimensionless vortex speed U^*. Filled symbols are for chimneys, and unfilled symbols are for orifices of various sizes. Experimental data from Sallet[1] are shown by circles.

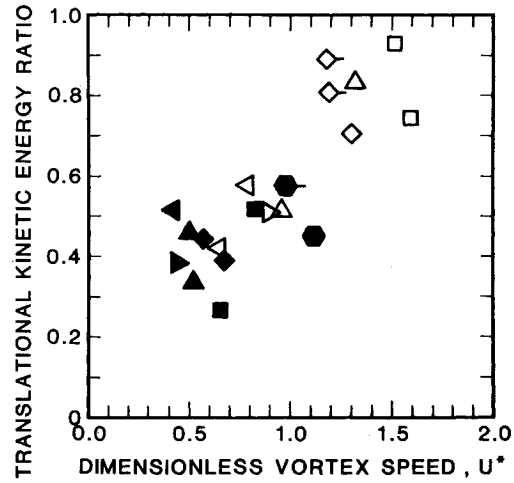

Fig. 4 Ratio of translational kinetic energy of vortex to the initial kinetic energy of the pulse vs dimensionless vortex speed U^*. Filled symbols are for chimneys, and unfilled symbols are for orifices of various sizes.

In summary, this work has shown the following:

1) The dimensionless translational to rotational speed ratio U^* is a very useful parameter for correlating vortex ring data.

2) Exit boundary conditions can have a very large effect on the entrainment and the partition of kinetic energies of translation and rotation.

3) Vortices with minimal amounts of kinetic energy of rotation can be generated by proper attention to boundary conditions and by using pulses of extremely short duration.

References

[1]Sallet, D. W. and Widmayer, R., "An Experimental Investigation of Laminar and Turbulent Vortex Rings in Air," *Zeitschrift für Flugwissenschaften*, Vol. 22, Heft 2, 1974.